Forest Chemicals Review
www.forestchemicalsreview.com
ISSN: 1520-0191
May-June 2022 Page No. 1913-1930
Article History: Received: 24 February 2022, Revised: 05 April 2022, Accepted: 08 May 2022, Publication: 30 June 2022

Research on 5G-R Modulation Interference Performance in Agricultural and Forestry Environment

Zhukai Shen[1*], Jinbai Zou[1], Aihuang Guo[2], Lidong Zhang[3]
[1]School of Railway Transportation, Shanghai Institute of Technology, Shanghai 201418, China
[2]School of Electronics and Information Engineering, Tongji University, Shanghai 201804, China
[3]Technical Center of Shanghai Shentong Metro Group Co., Ltd, Shanghai 201103, China
*Corresponding Author.

Abstract:

With the development of new services and new requirements of railway 5G special mobile communication network, a large number of communication equipment along the railway will be placed in a large area of agroforestry environment, and will inevitably be interfered by different modulation signals in different wireless communication systems. Therefore, it is of great significance to study the interference between different modulation signals. In this paper, the communication scene was firstly abstracted, a QAM demodulation model was established, and the error rate of 5G-R 64QAM modulation signal under additive White Gaussian noise (AWGN) was calculated by monte Carlo method. Secondly, the bit error rate formula of M-QAM under two-dimensional digital modulation interference was derived, and the influence of phase difference on interference performance was analyzed. Finally, the model simulation of 5G-R 64QAM system was carried out, and the influence of different M-QAM modulation signals on 64QAM demodulation was compared. The simulation results showed that quadrature phase shift keying (QPSK) has great influence on 64QAM demodulation performance, and different phase shifts have little influence on bit error rate. The conclusion of this study can provide theoretical support for the anti-interference performance of communication equipment along the line in agricultural and forestry environment, and has practical engineering value.

Keywords*: Agroforestry, 5G-R, Modulation, Interference, Bit error rate*

I. INTRODUCTION

With the vigorous development of high-speed railways (HSRS), railway communication has attracted great attention from academia and industry. At present, GSM-R (GSM for railway) is widely used as the train ground wireless communication network in the railway industry, but GSM-R belongs to 2G narrowband digital mobile communication technology, with small communication capacity and transmission rate, which can not meet the needs of the existing communication network [1]. Different from 5G in the mobile communication network, railway 5G-R system, as the successor of the future railway mobile communication system, not only retains all the technologies and functions of the original 5G system platform, but also

Forest Chemicals Review
www.forestchemicalsreview.com
ISSN: 1520-0191
May-June 2022 Page No. 1913-1930
Article History: Received: 24 February 2022, Revised: 05 April 2022, Accepted: 08 May 2022, Publication: 30 June 2022

expands the key business functions necessary for the railway industry, such as adding the special dispatching communication function for railway transportation, so as to be more suitable for complex scenes and harsh indicators in rail transit [2]. Moreover, train group call registers are added to the core network side to meet ultra-reliable train operation control signal transmission and high-quality user experience [3]. However, the construction of 5G-R network will not be accomplished at one stroke. In order to meet the communication requirements of various scenarios in the intelligent railway, the railway mobile communication system will be placed in a heterogeneous network [4]. It is expected to gradually realize mature and large-scale applications in 2030 [5]. As the railway wireless communication technology becomes more and more advanced, the corresponding network structure becomes more and more mature. For the railway linear network, the railway department pays close attention to the problem of realizing the stable transmission of wireless network through a large area of farmland and forest environment [6]. In addition, there are generally residential areas around the agriculture and forestry environment, and the civil or other wireless signals in this area will definitely cause signal interference to the special communication equipment placed in the agriculture and forestry environment, affecting the railway wireless communication service quality [7]. Therefore, it has certain theoretical significance and practical engineering value to study the impact of different interferences on the railway 5G-R wireless communication system in the agricultural and forestry environment.

The main baseband modulation method of 5G-R is Quadrature Amplitude Modulation (QAM). Through the combination of amplitude modulation and phase modulation, the bandwidth is doubled, thereby improving system efficiency. When the train is running, the modulated signals generated by different systems will inevitably interfere with each other, resulting in the increase of system bit error rate, which will affect the performance of 5G-R wireless communication system [8]. The modulation method has evolved from 3G to 5G. 3G has QPSK, 16QAM two modulation mode, the existing 4G has QPSK, 16QAM, 64QAM three amplitude modulation mode, 5G new air interface will continue to support 3G and 4G modulation mode, and add 256QAM modulation mode to improve the system capacity [9]. However, if different systems adopt different modulation methods, it is bound to cause signal interference between systems, reduce the performance of QAM system and even hinder communication, affecting the normal operation of trains [10]. The literature survey shows that the literature [11] analyzed and compared the performance efficiency of various QAM modulation schemes (QAM, 16QAM, 32QAM, 64QAM) when passing through noise/fading channel, and compared the bit error rate and bit energy noise of each communication scenario. Reference [12] used MATLAB/Simulink to simulate the digital modulation schemes (M-ary QAM and M-ary PSK) under additive white Gaussian noise (AWGN). The results showed that among the three modulation schemes, QAM had the best bit error rate performance and the lowest energy consumption. Reference [13] studied the theoretical bit error rate of M-QAM in different scenarios, gave a mathematical bit error rate formula, and verified the validity of the formula.

Since the agricultural and forestry environment along the railway is generally open and the channel characteristics are relatively stable, the channel model used in this paper is a Gaussian channel model, and the influence of the QAM interference signal on the demodulation performance of the 5G-R modulated signal is studied under this channel. Taking 64QAM as an example, firstly, the QAM demodulation model

Forest Chemicals Review
www.forestchemicalsreview.com
ISSN: 1520-0191
May-June 2022 Page No. 1913-1930
Article History: Received: 24 February 2022, Revised: 05 April 2022, Accepted: 08 May 2022, Publication: 30 June 2022

was established; Secondly, using Monte Carlo method, the symbol error rate of 5G-R 64QAM modulation signal under AWGN was calculated, and the general formula of M-QAM bit error rate under two-dimensional modulation was deduced; Finally, the modulation and demodulation model was established for verification, and the influence of different modulation interference on the demodulation performance of 64QAM was analyzed.

II. INTERFERENCE ANALYSIS OF RAILWAY 5G-R WIRELESS COMMUNICATION SYSTEM

5G-R network architecture adopts standalone (SA) networking mode, rather than transitional mode like non-standalone (NSA) networking. Different from 3GPP SA networking architecture, edge user plane function (UPF) is connected to mobile edge computing (MEC), which adds application service functions to 5G-R network and meets the needs of industry application business. As shown in Fig 1, 5G-R system architecture mainly includes six parts: core network (CN), radio access network (RAN), user equipment (UE), operation support systems (OSS), application business system and other communication systems [14].

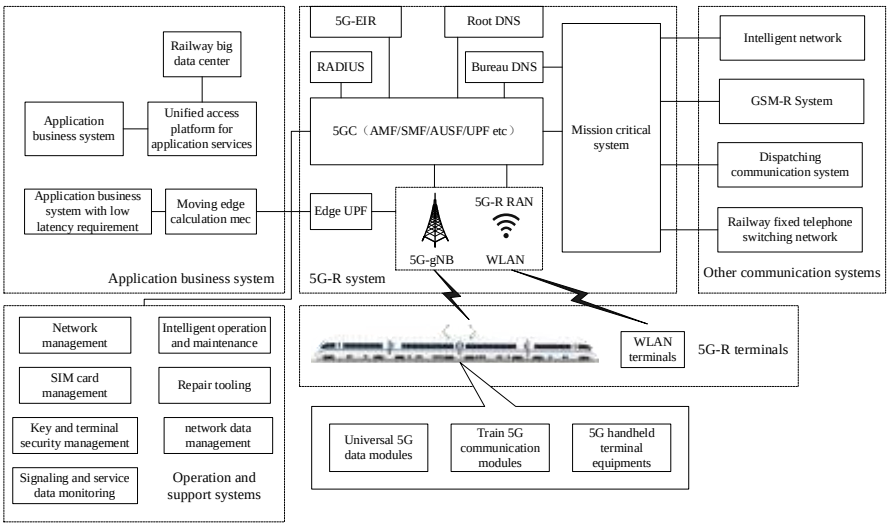

Fig 1: 5G-R network architecture

As a broadband digital mobile communication system, the communication quality of 5G-R depends on the physical basis of electromagnetic environment and coverage degree of field intensity. By detecting the electromagnetic environment, we can judge whether there is interference in the network operating environment and whether the signal-to-noise ratio meets the requirements of wireless signal sending and receiving [15]. At present, the railway 5G-R target frequency band (uplink 1965 ~ 1975MHz, downlink 2155 ~ 2165MHz) is adjacent to the frequency of China Unicom 4G communication system (uplink 1945 ~ 1965 MHz, downlink 2135 ~ 2155MHz), and there is a risk of electromagnetic interference between systems [16]. When the train and railway handheld terminals are located at the edge of 5G-R cell and in the center of the operator cell, their received signals are most seriously disturbed by the operator base station;

Forest Chemicals Review
www.forestchemicalsreview.com
ISSN: 1520-0191
May-June 2022 Page No. 1913-1930
Article History: Received: 24 February 2022, Revised: 05 April 2022, Accepted: 08 May 2022, Publication: 30 June 2022

When the operator user terminals are located at the edge of the operator cell and in the center of the railway 5G-R cell, the transmission power of the operator terminal is the largest and the interference to the signal reception of the railway base station is the most serious. Moreover, in the agricultural and forestry environment, some trees block the transmitted or received signals to strengthen the interference to the useful signals. The schematic diagram of the interference scene is shown in Fig 2.

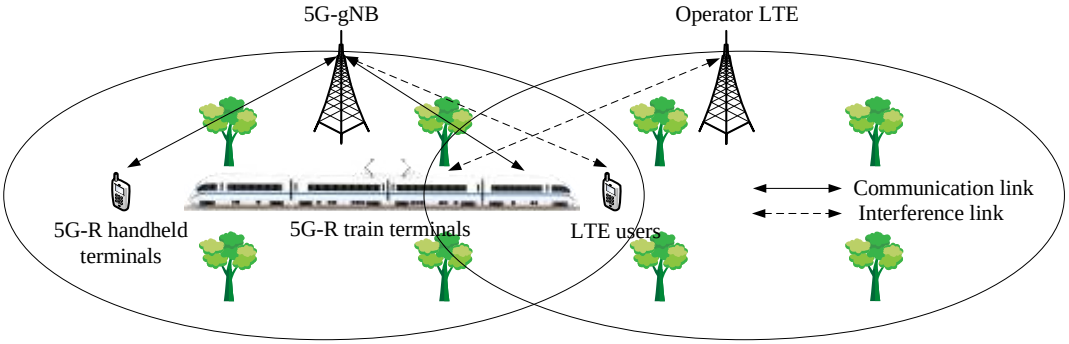

Fig 2: Scenario diagram of railway 5G-R system and operator network interference

In addition, when the train passes through the forest, 5G-R signals generated by each communication system are reflected through the forest and the surface of the car body, which degrades the signal reception performance and causes the same frequency interference between the systems. It can be seen that whether the adjacent frequency interference caused by the adjacent frequency operator network to 5G-R or the same frequency interference between systems will reduce the 5G-R demodulation performance, and then affect the safe operation of the train [17]. 5G-R system adopts QAM modulation. Although this modulation mode has high anti-noise ability, different QAM modulation signals of different systems will still influence each other.

III. ANALYSIS OF QAM DEMODULATION PERFORMANCE UNDER INTERFERENCE

Assuming that the modulation mode of the transmitted signal is known, the low-pass equivalent expression of the transmitted communication signal can be written as:

$$S(t)=\sum_{n=-\infty}^{\infty} P_s \boldsymbol{A}_n u(t-nT) \tag{1}$$

From formula above we can see, P_s represents the average power of the received communication signal; $u(t)$ represents the square root of the unit energy Nyquist pulse shape; $\boldsymbol{A}_n = A_{I,n} + jA_{Q,n}$ represents the data symbol of the known modulated signal in complex form within the symbol period, $A_{I,n}$ represents the in-phase component, $A_{Q,n}$ represents orthogonal components, j is an imaginary unit and obeys $F_A(a)$ distribution; T represents symbol width; t represents time.

Forest Chemicals Review
www.forestchemicalsreview.com
ISSN: 1520-0191
May-June 2022 Page No. 1913-1930
Article History: Received: 24 February 2022, Revised: 05 April 2022, Accepted: 08 May 2022, Publication: 30 June 2022

In the same way, the low-pass equivalent expression of the interference signal $\boldsymbol{J}(t)$ can be written as:

$$\boldsymbol{J}(t)=\sum_{k=-\infty}^{\infty} P_j \boldsymbol{J}_k u(t-kT) \tag{2}$$

In the formula, P_j represents the average power of the interfering signal; $\boldsymbol{J}_k$ represents the modulated symbol that conforms to a certain modulation method and obeys the $F_J(j)$ distribution.

Assuming that the background noise of the channel is AWGN, and the channel has no fading, the signal $\boldsymbol{r}_m$ received by the receiver can be expressed as:

$$\boldsymbol{r}_m=\boldsymbol{r}(t=mT)=\left(P_s\boldsymbol{A}_m+P_j\boldsymbol{J}_m\right)e^{j\omega_0 t}+n_m \tag{3}$$

In the formula, n_m is gaussian white noise with mean value 0 and variance σ^2. The modulated signal $\boldsymbol{A}_m$, the interference modulated symbol $\boldsymbol{J}_m$ and the Gaussian white noise n_m are independent.

3.1 Calculate the Average Energy of M-QAM

In the process of M-QAM modulation, different modulation modes have different energies. In order to make all mappings have the same average power, the mapped complex numbers need to be normalized to obtain the output data [18]. The value of the normalization factor varies according to the modulation modes, and for an M-QAM constellation map, $\sqrt{M}$ is a power of 2 [19]. Therefore, the coordinate expression for each symbol on the constellation diagram is:

$$\boldsymbol{\alpha}_{M-QAM}=\pm(2m-1)\pm(2m-1)\mathrm{j}, m\in\left\{1,2,\cdots,\frac{\sqrt{M}}{2}\right\} \tag{4}$$

Taking advantage of the symmetry of the constellation diagram, note that each quadrant contains $M/4$ constellation points, and the energy of the real and imaginary components is the same. Furthermore, the elements of each symbol in each quadrant are used $\sqrt{M}/2$ times by the real and imaginary parts. Therefore, the average energy in the M -ary constellation can be expressed as:

$$E_{M-QAM}=\varepsilon\left\{\mathrm{Re}\left|\boldsymbol{\alpha}_{M-QAM}\right|^2\right\}+\varepsilon\left\{\mathrm{Im}\left|\boldsymbol{\alpha}_{M-QAM}\right|^2\right\}=\frac{2\frac{\sqrt{M}}{2}}{\frac{M}{4}}\sum_{m=1}^{\frac{\sqrt{M}}{2}}(2m-1)^2=\frac{2}{3}(M-1) \tag{5}$$

Forest Chemicals Review
www.forestchemicalsreview.com
ISSN: 1520-0191
May-June 2022 Page No. 1913-1930
Article History: Received: 24 February 2022, Revised: 05 April 2022, Accepted: 08 May 2022, Publication: 30 June 2022

3.2 Under AWGN Condition, 64QAM Error Symbol Rate

Monte Carlo method is used to sample random samples and estimate the probability with the frequency of random events, so as to transform the bit error problem into a characteristic number of random distribution for solution [20]. Taking the study of 64QAM symbol error rate as an example, assuming that the average energy of each symbol is E_s and the equal probability occurs, the average energy of the 64QAM constellation is $E_{64QAM} = 42$. The constellation diagram of 64QAM is shown in

Fig 3. It can be seen from the figure that each symbol point has a corresponding average energy of $\sqrt{E_s / 42}$.

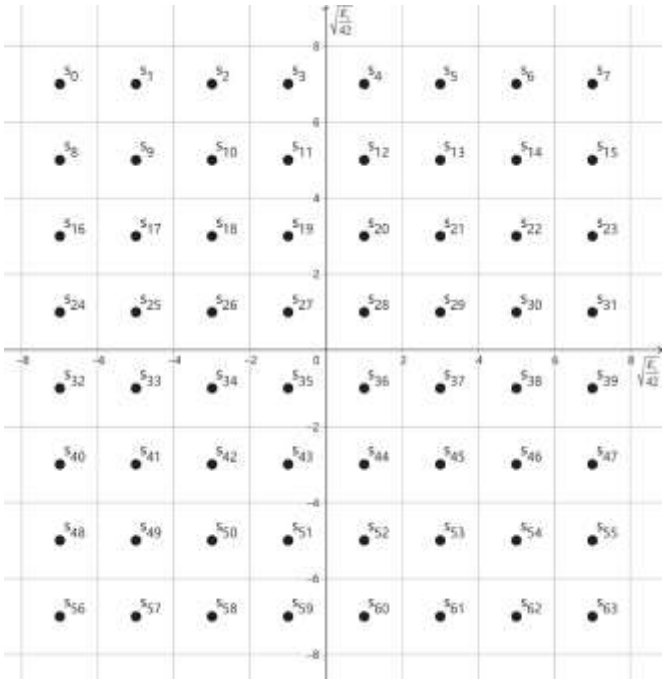

Fig 3: 64QAM constellation diagram

Because different symbols have different positions in the constellation diagram and have different energies, three different symbol types need to be discussed in order to determine the symbol error rate. The corner symbol area is $\{S_0, S_7, S_{56}, S_{63}\}$, the inner area is $\{S_9, S_{10}, S_{11}, S_{12}, S_{13}, S_{14}, S_{17}, S_{18}, S_{19}, S_{20}, S_{21}, S_{22}, S_{25}, S_{26}, S_{27}, S_{28}, S_{29}, S_{30}, S_{33}, S_{34}, S_{35}, S_{36}, S_{37}, S_{38}, S_{41}, S_{42}, S_{43}, S_{44}, S_{45}, S_{46}, S_{49}, S_{50}, S_{51}, S_{52}, S_{53}, S_{54}\}$, and the rest of the symbols have the same constraints, neither in the interior nor in the corner, and the area is $\{S_1, S_2, S_3, S_4, S_5, S_6, S_{15}, S_{23}, S_{31}, S_{39}, S_{47}, S_{55}, S_{57}, S_{58}, S_{59}, S_{60}, S_{61}, S_{62}, S_8, S_{16}, S_{24}, S_{32}, S_{40}, S_{48}\}$.

Because it is symmetrical, the contribution of each symbol in the three sets to the bit error rate is the same. Let $S_0 \square S_{63}$ be the transmitting signal, r the receiving signal, the background noise of the channel is AWGN, and there is no channel fading. The expression of the received signal is:

Forest Chemicals Review
www.forestchemicalsreview.com
ISSN: 1520-0191
May-June 2022 Page No. 1913-1930
Article History: Received: 24 February 2022, Revised: 05 April 2022, Accepted: 08 May 2022, Publication: 30 June 2022

$$r = S_i + n, i = 0,1\cdots,63 \tag{6}$$

In the formula: S_i is the i th transmitted signal, n is a Gaussian random variable, and the probability density function is:

$$P_n(x) = \frac{1}{\sqrt{2\pi}\sigma} e^{-\frac{(x-\mu)^2}{2\sigma^2}} \tag{7}$$

In the formula: x is a random variable; $\mu = 0$, $\sigma^2 = N_0/2$ and N_0 are the power spectral densities of Gaussian white noise.

Assuming that the probability density function of transmitter S_7 and receiver $r(t)$ is:

$$P\left[r(t)|S_7\right] = \frac{1}{\sqrt{\pi N_0}} e^{-\frac{(r-\mu_1)^2}{N_0}} \tag{1}$$

In the formula: μ_1 represents the average energy of emission S_7.

As shown in Fig 4, only when $r(t)$ falls into the shaded area around S_7, the decoding is correct. At this time, the probability of the receiving end correctly receiving S_7 is:

$$\Pr\left[c|S_7\right] = \Pr\left\{\mathrm{Re}\left\{r(t) > 6\sqrt{\frac{E_s}{42}}\right\}|S_7\right\} \cdot \Pr\left\{\mathrm{Im}\left\{r(t) > 6\sqrt{\frac{E_s}{42}}\right\}|S_7\right\} \tag{2}$$

Forest Chemicals Review
www.forestchemicalsreview.com
ISSN: 1520-0191
May-June 2022 Page No. 1913-1930
Article History: Received: 24 February 2022, Revised: 05 April 2022, Accepted: 08 May 2022, Publication: 30 June 2022

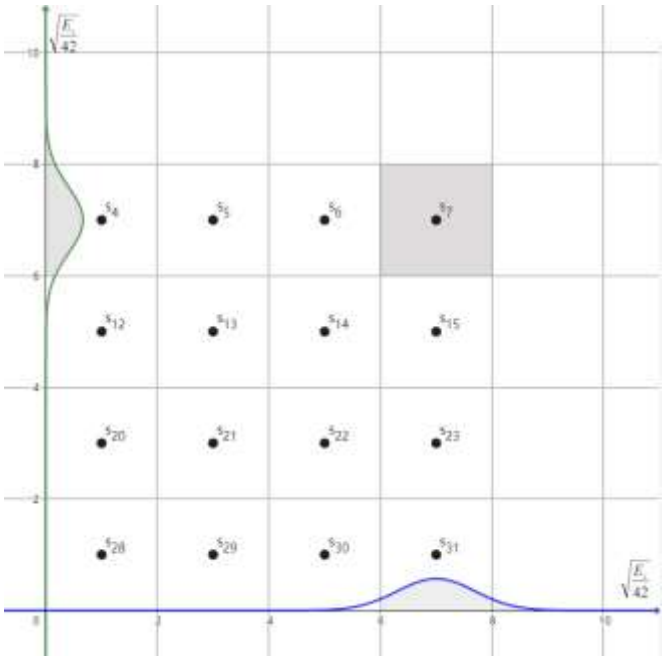

Fig 4: Constellation diagram correctly receives the area of S_7

Assuming that $\mathrm{Re}\{r(t)\}$ and $\mathrm{Im}\{r(t)\}$ are independent of each other, there are:

$$\Pr[c|S_7] = \left[\frac{1}{\sqrt{\pi N_0}} \int_{6\sqrt{\frac{E_s}{42}}}^{\infty} e^{-\frac{\left(x-7\sqrt{\frac{E_s}{42}}\right)^2}{N_0}} dx\right]^2 = \left[1-\frac{1}{2}erfc\left(\sqrt{\frac{E_s}{42N_0}}\right)\right]^2 \quad (10)$$

In the formula: $erfc(x)$ represents the error function.

Therefore, the probability of incorrect B decoding is:

$$\overline{\Pr}[c|S_7] = 1-\Pr[c|S_7] = 1-\left[1-\frac{1}{2}erfc\left(\sqrt{\frac{E_s}{42N_0}}\right)\right]^2 \approx erfc\left(\sqrt{\frac{E_s}{42N_0}}\right) \quad (11)$$

Secondly, consider the symbols inside the constellation, such as S_{14}.Using the same steps above, when $r(t)$ falls into the shadowed area around S_{14}, the symbol S_{14} can be decoded correctly, as shown in Fig 5. At this time, the probability of correct reception by the receiver S_{14} is:

Forest Chemicals Review
www.forestchemicalsreview.com
ISSN: 1520-0191
May-June 2022 Page No. 1913-1930
Article History: Received: 24 February 2022, Revised: 05 April 2022, Accepted: 08 May 2022, Publication: 30 June 2022

$$\Pr\left[c\left|S_{14}\right.\right]=\left[1-erfc\left(\sqrt{\frac{E_s}{42N_0}}\right)\right]^2 \tag{12}$$

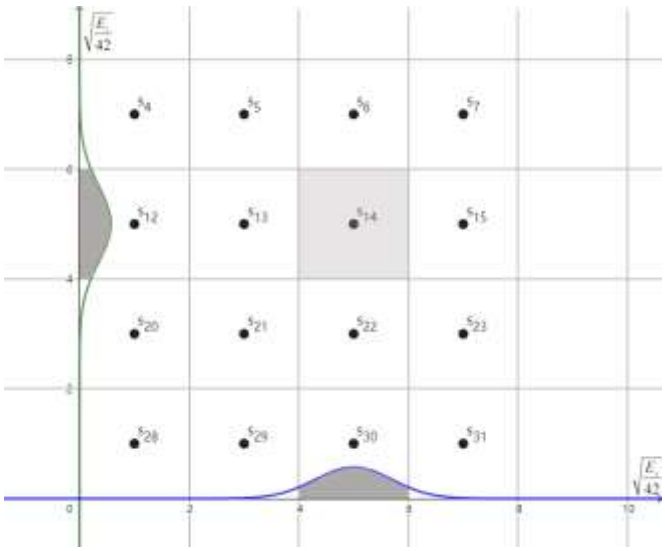

Fig 5: Constellation diagram correctly receives the area of S_{14}

The probability that S_{14} cannot decode correctly is:

$$\overline{\Pr}\left[c\left|S_{14}\right.\right]=1-\Pr\left[c\left|S_{14}\right.\right]=1-\left[1-erfc\left(\sqrt{\frac{E_s}{42N_0}}\right)\right]^2\approx 2erfc\left(\sqrt{\frac{E_s}{42N_0}}\right) \tag{3}$$

Finally, consider symbols that are neither on the Angle nor inside, such as S_{15}. when $r(t)$ falls into the shadowed area around S_{15}, the symbol S_{15} can be decoded correctly, as shown in

Fig 6. At this time, the probability of correct reception by the receiver S_{15} is:

$$\Pr\left[c\left|S_{15}\right.\right]=\left[1-\frac{1}{2}erfc\left(\sqrt{\frac{E_s}{42N_0}}\right)\right]\cdot\left[1-erfc\left(\sqrt{\frac{E_s}{42N_0}}\right)\right] \tag{4}$$

Forest Chemicals Review
www.forestchemicalsreview.com
ISSN: 1520-0191
May-June 2022 Page No. 1913-1930
Article History: Received: 24 February 2022, Revised: 05 April 2022, Accepted: 08 May 2022, Publication: 30 June 2022

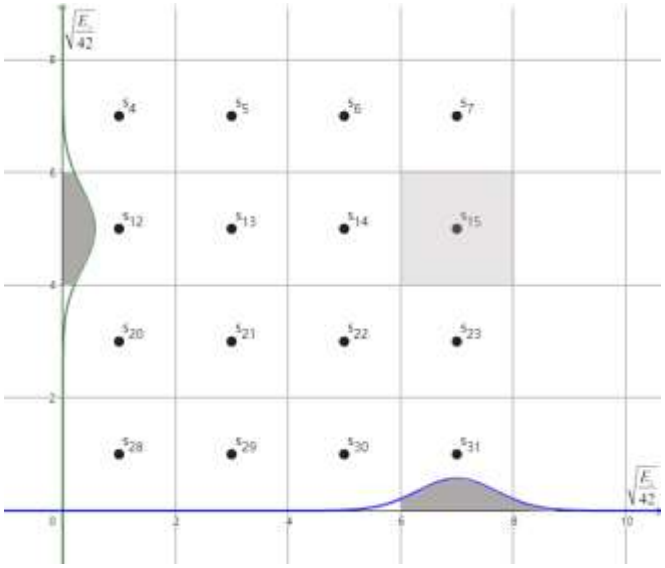

Fig 6: Constellation diagram correctly receives the area of S_{15}

The probability that S_{15} cannot decode correctly is:

$$\overline{\Pr}\left[c\middle|S_{15}\right]=1-\Pr\left[c\middle|S_{15}\right]=1-\left[1-\frac{1}{2}erfc\left(\sqrt{\frac{E_s}{42N_0}}\right)\right]\cdot\left[1-erfc\left(\sqrt{\frac{E_s}{42N_0}}\right)\right]\approx\frac{3}{2}erfc\left(\sqrt{\frac{E_s}{42N_0}}\right) \quad (15)$$

To sum up, assuming that all symbols have equal probability (4 in the corner, 36 in the middle and 24 in other positions), the total symbol error rate of 64QAM is:

$$P_{e,64QAM}\approx\frac{4}{64}\cdot erfc\left(\sqrt{\frac{E_s}{42N_0}}\right)+\frac{36}{64}\cdot 2erfc\left(\sqrt{\frac{E_s}{42N_0}}\right)+\frac{24}{64}\cdot\frac{3}{2}erfc\left(\sqrt{\frac{E_s}{42N_0}}\right)\approx\frac{7}{4}erfc\left(\sqrt{\frac{E_s}{42N_0}}\right) \quad (16)$$

IV. GENERAL FORMULA OF BIT ERROR RATE OF M-QAM UNDER TWO-DIMENSIONAL MODULATION

In the M-QAM rectangular signal constellation, it can be equivalent to two PAM signals on the orthogonal carrier, each of which has $\sqrt{M}$ signal points [21]. Since the signal components with orthogonal phase can be completely separated by coherent detection, the error probability of QAM can be easily determined by the error probability of pulse amplitude modulation (PAM). In M-PAM modulation, the minimum Euclidean distance $d_{\min}$ of any two points [22] is defined as:

$$d_{\min}=\sqrt{\frac{12E_s}{M^2-1}} \quad (17)$$

Forest Chemicals Review
www.forestchemicalsreview.com
ISSN: 1520-0191
May-June 2022 Page No. 1913-1930
Article History: Received: 24 February 2022, Revised: 05 April 2022, Accepted: 08 May 2022, Publication: 30 June 2022

For one-dimensional PAM signal, the probability of error at $M-2$ inner points (excluding the points of two endpoints) is:

$$P_{ei}=P\left[\left|r-s_m\right|>\frac{d_{\min}}{2}\right]=2Q\left(\frac{d_{\min}}{\sqrt{2N_0}}\right) \tag{18}$$

In the formula: $Q(x)$ is the function of the area under the tail of the Gauss curve.

Since noise only works in one direction, the error rate of the two endpoints is half of that of the inner point, so:

$$P_{eo}=Q\left(\frac{d_{\min}}{\sqrt{2N_0}}\right) \tag{19}$$

Assuming that all points on the constellation have equal probability, the total symbol error probability is:

$$P_e=\frac{M-2}{M}\cdot 2Q\left(\frac{d_{\min}}{\sqrt{2N_0}}\right)+\frac{2}{M}\cdot Q\left(\frac{d_{\min}}{\sqrt{2N_0}}\right)=\frac{2(M-1)}{M}Q\left(\frac{d_{\min}}{\sqrt{2N_0}}\right) \tag{20}$$

Combine equations (17) and (20) to obtain:

$$P_e=\frac{2(M-1)}{M}Q\left(\sqrt{\frac{6E_s}{(M^2-1)N_0}}\right)=2\left(1-\frac{1}{M}\right)Q\left(\sqrt{\frac{6E_b\log_2 M}{(M^2-1)N_0}}\right) \tag{21}$$

In the formula: E_b is the average bit energy.

Since QAM signal can be regarded as the combination of two PAM signals, the error probability of QAM signal can be calculated by using PAM signal error probability.

Assuming that the error probability of each $\sqrt{M}$ -ary PAM is:

$$P_{\sqrt{M}-PAM}=2\left(1-\frac{1}{\sqrt{M}}\right)Q\left(\sqrt{\frac{3E_b\log_2 M}{(M-1)N_0}}\right) \tag{22}$$

The probability of correct judgment is:

$$P_c=\left(1-P_{\sqrt{M}-PAM}\right)^2 \tag{23}$$

Forest Chemicals Review
www.forestchemicalsreview.com
ISSN: 1520-0191
May-June 2022 Page No. 1913-1930
Article History: Received: 24 February 2022, Revised: 05 April 2022, Accepted: 08 May 2022, Publication: 30 June 2022

In the absence of interference, the error sign probability of M-QAM is:

$$P_{M-QAM}=1-\left(1-P_{\sqrt{M}-PAM}\right)^2=4\left(1-\frac{1}{\sqrt{M}}\right)Q\left(\sqrt{\frac{3E_b\log_2 M}{(M-1)N_0}}\right)\cdot\left[1+\left(1-\frac{1}{\sqrt{M}}\right)Q\left(\sqrt{\frac{3E_b\log_2 M}{(M-1)N_0}}\right)\right] \quad (24)$$

When there is an interfering signal in M-QAM, in the same dimension, the signal received by the receiver is:

$$x(t)=2\int_0^T \boldsymbol{r}_m(t)\cos(\omega_0 t)dt=2\int_0^T P_s\boldsymbol{A}_m\cos^2(\omega_0 t)dt+2\int_0^T P_j\boldsymbol{J}_m\cos^2(\omega_0 t)dt+2\int_0^T \boldsymbol{n}_m\cos^2(\omega_0 t)dt \quad (25)$$

In the formula: $\boldsymbol{r}_m$ represents the received signal symbol; $\boldsymbol{A}_m$ represents the modulated signal symbol; $\boldsymbol{n}_m$ represents the Gaussian white noise with zero mean value; $\boldsymbol{J}_m$ represents the interference signal with mean $J(t)$ and variance N_0, and the probability density is:

$$f(x)=\frac{1}{\sqrt{2\pi N_0}}\mathrm{e}^{-\frac{[x-J(t)]^2}{2N_0}} \quad (26)$$

When the source sends "0" and "1" with equal probability, the bit error rate of a certain dimension can be expressed as:

$$P_{e\_jam}=\frac{1}{2}\left[Q\left(\sqrt{\frac{6E_b\log_2 M}{(M^2-1)N_0}}+\frac{J(t)}{\sqrt{N_0}}\right)+Q\left(\sqrt{\frac{6E_b\log_2 M}{(M^2-1)N_0}}-\frac{J(t)}{\sqrt{N_0}}\right)\right] \quad (27)$$

Since the mapping of interference signal $\boldsymbol{J}_m$ in a single dimension is not unique, in order not to lose generality, the above formula is modified as follows:

$$P_{e\_jam}=\sum_{m=1}^{L}\left\{Q\left(\sqrt{\frac{6E_b\log_2 M}{(M^2-1)N_0}}+\frac{\boldsymbol{J}_m(t)}{\sqrt{N_0}}\right)+Q\left(\sqrt{\frac{6E_b\log_2 M}{(M^2-1)N_0}}-\frac{\boldsymbol{J}_m(t)}{\sqrt{N_0}}\right)\right\}\frac{1}{2L} \quad (28)$$

In the formula: L is the number of mappings in a single dimension (if M =64, then L =6).
Therefore, in the presence of interference, the error symbol probability P_{e_all} of M-QAM is:

$$P_{e\_all}=1-\left(1-P_{e\_jam}\right)^2 \quad (29)$$

Forest Chemicals Review
www.forestchemicalsreview.com
ISSN: 1520-0191
May-June 2022 Page No. 1913-1930
Article History: Received: 24 February 2022, Revised: 05 April 2022, Accepted: 08 May 2022, Publication: 30 June 2022

V. EFFECT OF PHASE DIFFERENCE ON BIT ERROR RATE OF M-QAM UNDER INTERFERENCE

Assuming that there is a random phase difference φ between the interference signal and the communication signal, the signal $\boldsymbol{r}_m$ received by the receiver is expressed as:

$$\boldsymbol{r}_m = \boldsymbol{r}\left(t = mT\right) = \left(P_s \boldsymbol{A}_m + P_j \boldsymbol{J}_m \mathrm{e}^{i\varphi}\right)\mathrm{e}^{j\omega_0 t} + \boldsymbol{n}_m, m = 1,2,3\cdots \tag{30}$$

In the formula: the random phase offset φ follows the uniform distribution of $0 \sim 2\pi$.

It can be seen from the derivation in the previous chapter that the bit error rate of any dimension can be expressed as:

$$\begin{aligned} P_{e\_phase} = \frac{1}{L}\sum_{m=1}^{L}\left\{\frac{1}{2}\left[Q\sqrt{\frac{6E_b \log_2 M}{\left(M^2-1\right)N_0}} + \frac{\boldsymbol{J}_m(t)}{\sqrt{N_0}}\left(\mathrm{Re}\cos\varphi + \mathrm{Im}\sin\varphi\right) + \right.\right. \\ \left.\left. Q\sqrt{\frac{6E_b \log_2 M}{\left(M^2-1\right)N_0}} - \frac{\boldsymbol{J}_m(t)}{\sqrt{N_0}}\left(\mathrm{Re}\cos\varphi + \mathrm{Im}\sin\varphi\right)\right]\right\} \end{aligned} \tag{31}$$

To sum up, in the presence of phase-shift interference, the error symbol probability of M-QAM is:

$$P_{phase\_all} = 1 - \left(1 - P_{e\_phase}\right)^2 \tag{32}$$

VI. SIMULATION AND RESULT ANALYSIS

The 5G-R 64QAM simulation system was built by using MATLAB software. Firstly, demodulated different modulated signals, observed whether the simulated bit error rate was consistent with the theoretical bit error rate, and verified the correctness of the simulation system; Secondly, considering that LTE has QPSK, 16QAM, 64QAM, 256qam and other modulation modes, these signals with different modulation modes are used as interference sources to interfere with 5G-R 64QAM signals. Assuming that there was no fading in the channel of the simulation system, the channel noise was Gaussian white noise, the communication signal transmitter and noise transmitter adopted gray coding system, and the transmission power of the interference signal was less than that of the interfered signal, Observing the error code curve of communication signal; Finally, observed the impact of bit errors when there was a random phase difference between the interfering signal and the system signal. The signal and interference carrier frequencies used in the simulation experiments were both 2.1GHz.

Forest Chemicals Review
www.forestchemicalsreview.com
ISSN: 1520-0191
May-June 2022 Page No. 1913-1930
Article History: Received: 24 February 2022, Revised: 05 April 2022, Accepted: 08 May 2022, Publication: 30 June 2022

Fig 7 showed that the receiving points of four modulation signals were randomly distributed around the standard constellation points, which proved that the four modulation signals transmitted in the simulation system were consistent with the signal transmission in the actual environment.

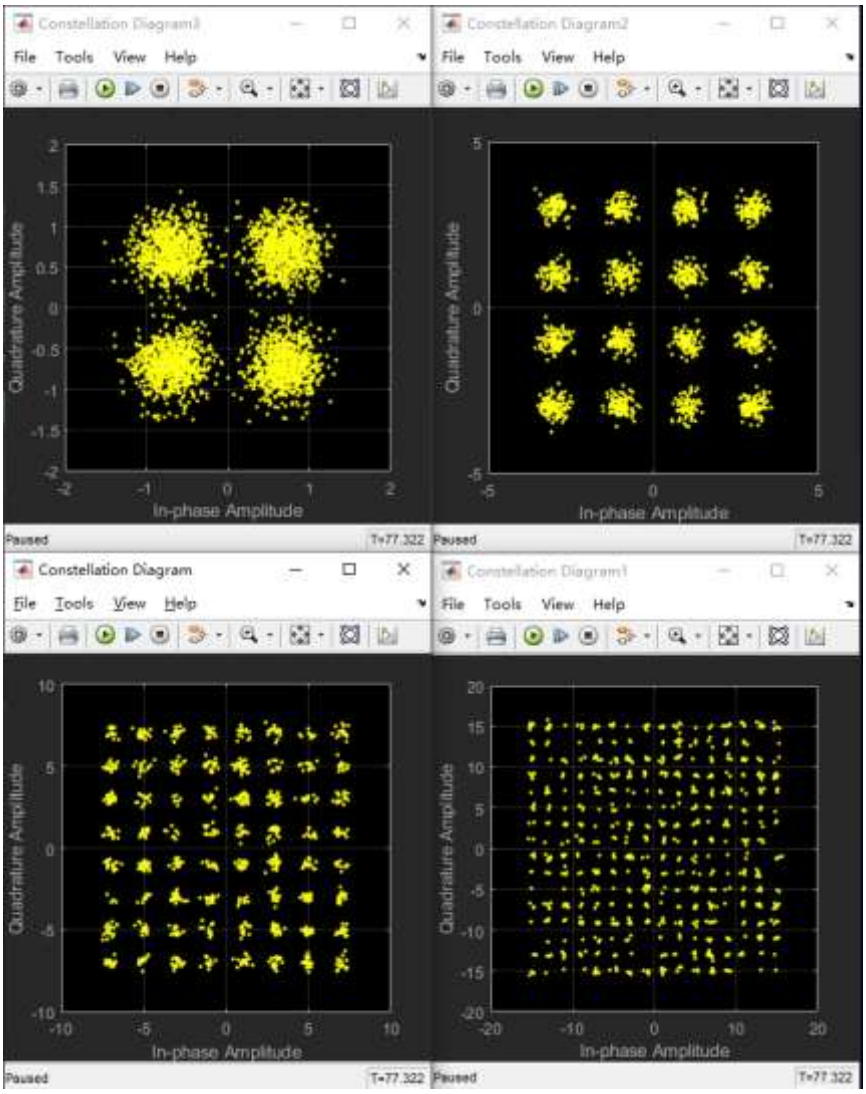

Fig 7: Receiving constellation diagram of four kinds of modulation signals

Fig 8 showed the comparison curve of the bit error rate between the theoretical value and the actual value of QPSK, 16QAM, 64QAM and 256QAM. The abscissa was the signal-to-noise ratio and the ordinate is the bit error rate. Under these four modulation modes, the theoretical ber curve of the received signal overlapped with the actual ber curve, which proved the correctness of the simulation system.

Forest Chemicals Review
www.forestchemicalsreview.com
ISSN: 1520-0191
May-June 2022 Page No. 1913-1930
Article History: Received: 24 February 2022, Revised: 05 April 2022, Accepted: 08 May 2022, Publication: 30 June 2022

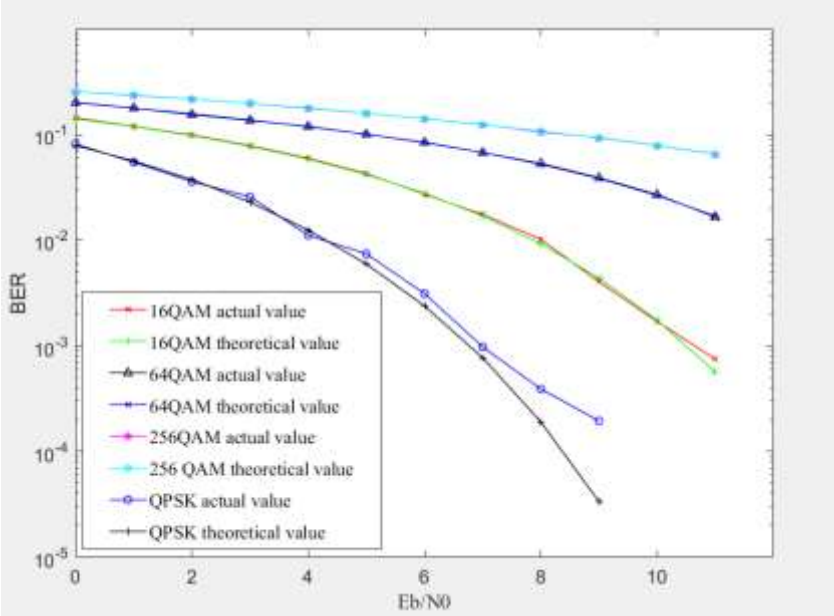

Fig 8: M-QAM signal interference theory and actual bit error rate curve

Fig 9 showed QPSK, 16QAM, 64QAM and 256QAM as interference signals, and the demodulation performance of 64QAM was obtained through coherent demodulation. It could be seen from the figure that when the bit energy noise was less than 4dB, the influence of different QAM modulation interference on the reception of 64QAM was not very obvious; When the bit energy noise started from 6dB, the impact of QPSK interference on 64QAM modulation communication signal was greater than that of each M-QAM modulation interference, and each M-QAM modulation interference signal had little impact on the demodulation and transmission performance of 64QAM.

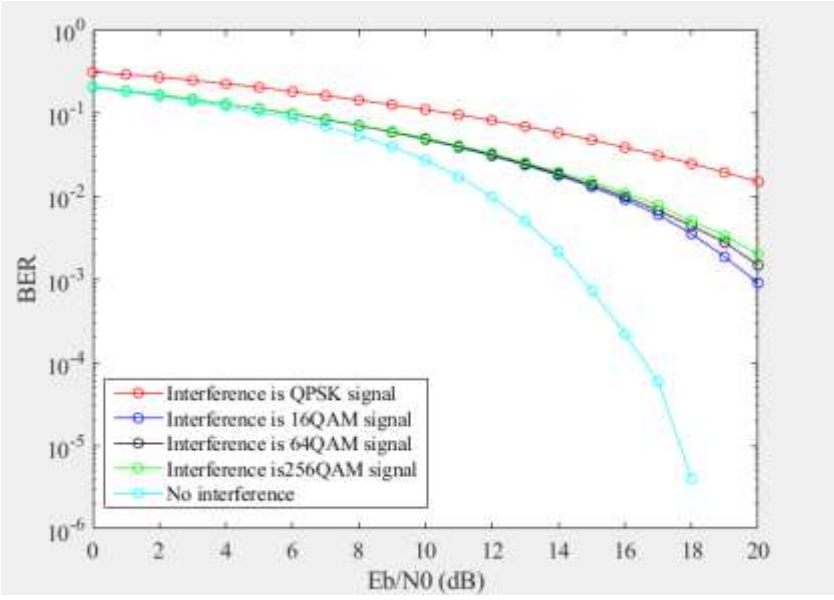

Fig 9: Four kinds of interference on the bit error rate curve of 64QAM system

Forest Chemicals Review
www.forestchemicalsreview.com
ISSN: 1520-0191
May-June 2022 Page No. 1913-1930
Article History: Received: 24 February 2022, Revised: 05 April 2022, Accepted: 08 May 2022, Publication: 30 June 2022

Fig 10 showed the receiving curve of the receiver when there was a random phase difference between the communication signal and the interference signal under the interference of the QPSK signal in 64QAM. Among them, when the bit energy noise was certain, the interference signal with phase difference of 0、$\pi/8$、$\pi/4$、$\pi/2$ in turn had little effect on the bit error rate of 64QAM.

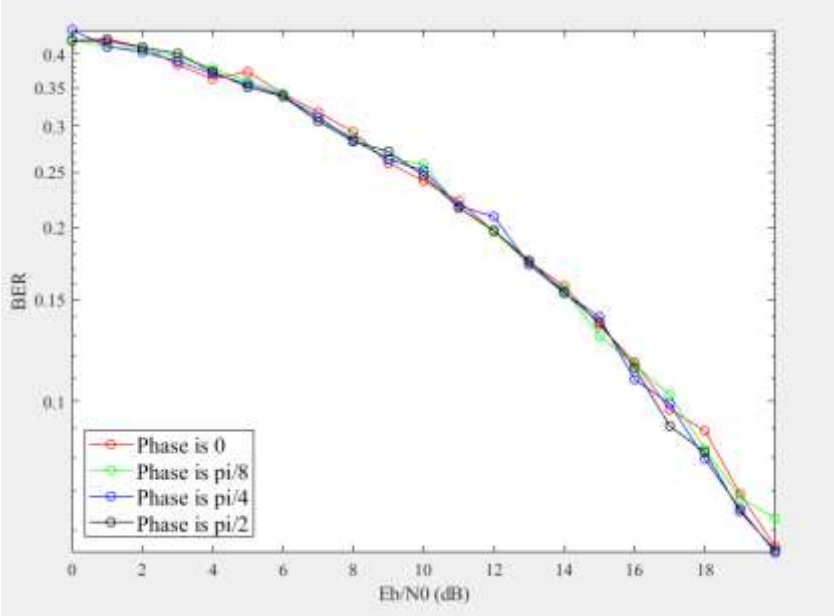

Fig 10: Bit error rate of QPSK with phase difference to 64QAM system

VII. CONCLUSION

This paper studied the influence of different modulation signals on the demodulation performance of 5G-R 64QAM signal in AWGN channel. The simulation results showed that when the bit energy noise was less than 4dB, the influence of different QAM modulation interference on the reception of 64QAM was not obvious; When the bit energy noise started from 6dB, the impact of QPSK interference on 64QAM modulation communication signal was greater than that of each M-QAM modulation interference, and each M-QAM modulation interference signal had little impact on the demodulation and transmission performance of 64QAM, and different phase shifts had little impact on the bit error rate. This paper only analyzed the interference between different modulation signals in Gaussian channel. However, in practical engineering,

However, in practical engineering, complex agriculture and forestry environment will make channel analysis more difficult. For example, in the open farmland environment, there is a single direct main path due to less shielding, so the description of Ricean channel is more appropriate. In the forest environment, Rayleigh channel is more appropriate because there are a lot of shielding and no direct path signal reaches the receiving end. Therefore, the future research of 5G-R wireless communication system can be further studied from different channel types, such as Rayleigh channel, Ricean channel and so on.

Forest Chemicals Review
www.forestchemicalsreview.com
ISSN: 1520-0191
May-June 2022 Page No. 1913-1930
Article History: Received: 24 February 2022, Revised: 05 April 2022, Accepted: 08 May 2022, Publication: 30 June 2022

ACKNOWLEDGEMENTS

This research was supported by 1) The Shanghai Science and Technology Commission "Research on Key Technologies of Intelligent Rail Transit Operation and Maintenance" (20090503100); 2) Research on Key Technologies of Massive MIMO Antenna in Rail Transit Tunnel Environment of the Open Project of Millimeter Wave State Key Laboratory (K201935); 3) "The Belt and Road" China-Laos Railway Engineering International Joint Laboratory (21210750300).

REFERENCES

[1] Chen Y, Chen Y. Analysis of LTE-R train-to-train communication delay for next generation high speed railway. Journal of Railway Science and Engineering, 2021, 18(08): 1997-2005.
[2] Li X, Xu Y. Research on 5G-R Signaling Networking Scheme. Railway Signalling & Communication Engineering, 2020, 17(10): 33-36.
[3] Ai B, Molisch A F, Rupp M, et al. 5G key technologies for smart railways. Proceedings of the IEEE, 2020, 108(6): 856-893.
[4] Li C R, Xie J L, Gao W J. Heterogeneous Network Access Technologies Based on 5G-R Services for High-Speed Railway. ZTE Technology Journal, 2021, 27(04): 18-23.
[5] Sun L Q, Shan H Z, Zhao J, et al. Study on Transition Solution to Voice Service from GSM-R and 5G-R. Railway Signalling & Communication, 2021, 57(10): 75-80.
[6] Li X M, Yang W X. Application summary of 5G communication in smart agriculture. Communication & Information Technology, 2021(03): 112-115.
[7] Wang Z G. High-speed rail wireless communication interference detection and identification technology. Telecom World, 2020, 27(04): 74-75.
[8] Zhang K B, Zou J B, Zhang H J. Influence of Different Modulation Interference on LTE-M Performance. Urban Mass Transit, 2020, 23(08): 143-147.
[9] Liu Y, Liu H M, Zhang Y, et al. Explain 5G Mobile Communications in a Simple Way. BeiJing: Machinery Industry Press, 2019: 39.
[10] Qin W, Wang K R, Jin H, et al. Effects of Different Jams on QAM Demodulation Performance. Communications Technology, 2016, 49(09): 1109-1114.
[11] Jirnadu T I, Ajibesin A A, Ishaq A T. Comparative Analysis of QAM Modulation Techniques over AWGN and Fading Channels//Advances in Science and Technology. Trans Tech Publications Ltd, 2021, 107: 194-200.
[12] Balarabe A T, Rufa'i A, Hassan Z L, et al. A Comprehensive Analysis of M-ary PSK and M-ary QAM Schemes. Asian Journal of Research in Computer Science, 2021: 63-71.
[13] Lu D, Zhou X, Yang Y, et al. Theoretical analysis of PAM-N and M-QAM BER computation with single-sideband signal. Information Sciences, 2021, 64(182312): 1-182312.
[14] Yang R, Guo G F, Zhao W Y. Research on Technical Scheme for Operation and Maintenance of 5G-R. China Railway, 2021(08): 19-25.
[15] Zhou H W. Research on Network Inspection System of 5G-R. China Academy of Railway Sciences, 2021.
[16] Mang Y, Li Y, Jiang Z Y. Research on Electromagnetic Interference Between Wayside LTE and 5G Mobile Communication Systems. 2021(08): 7-12.
[17] Duan B, Li C, Xie J, et al. Fast Handover Algorithm Based on Location and Weight in 5G-R Wireless Communications for High-Speed Railways. Sensors, 2021, 21(9): 3100.

Forest Chemicals Review
www.forestchemicalsreview.com
ISSN: 1520-0191
May-June 2022 Page No. 1913-1930
Article History: Received: 24 February 2022, Revised: 05 April 2022, Accepted: 08 May 2022, Publication: 30 June 2022

[18] Yu Z X, Xiao S L, Hou Y N, et al. Simulation of adaptive OFDM visible light communication system based on FPGA. Optical Communication Technology, 2015, 39(02): 24-27.
[19] Richard A. Poisel. Modern Communication Interference Principle and Technology. BeiJing: Electronics Industry, 2014.9.
[20] Chen M Y. AlphaGo and AlphaZero principle and future application research. Telecom World, 2019, 26(12): 22-23.
[21] Liu X Y. Detailed explanation of MATALB, Simulink communication system modeling and simulation. BeiJing: Electronics Industry, 2011.11.
[22] Sun Z G, Xu T Y, Deng C, et al. Analysis on Optimal Jamming Gainst 16-QAM Signal. Journal of Harbin Engineering University, 2018, 39(07): 1245-1250.